rpth
research & practice
in thrombosis & haemostasis

ORIGINAL ARTICLE

Measuring ADAMTS-13 activity to diagnose thrombotic thrombocytopenic purpura: a novel, fast fiber-optic surface plasmon resonance immunoassay

Quintijn Bonnez[1] | Charlotte Dekimpe[1] | Edwige Tellier[2] | Gilles Kaplanski[2,3] | Peter Verhamme[4] | Claudia Tersteeg[1] | Simon F. De Meyer[1] | Jeroen Lammertyn[5] | Bérangère Joly[6] | Paul Coppo[7] | Agnès Veyradier[6,8] | Karen Vanhoorelbeke[1]

[1]Laboratory for Thrombosis Research, IRF Life Sciences, KU Leuven Campus Kulak Kortrijk, Kortrijk, Belgium

[2]Aix-Marseille University, Institut National de la Santé et de la Recherche Médicale, INRAE, C2VN, Marseille, France

[3]Service de Médecine Interne et Immunologie Clinique, CHU Conception, Aix-Marseille University, APHM, Marseille, France

[4]Department of Cardiovascular Sciences, KU Leuven, Leuven, Belgium

[5]Department of Biosystems, Biosensors Group, KU Leuven, Leuven, Belgium

[6]Service d'Hématologie Biologique Hôpital Lariboisière, AP-HP and EA3518, IRSL, Université Paris Cité, Paris France

[7]Department of Hematology, Reference Center for Thrombotic Microangiopathies (CNR-MAT), Saint-Antoine University Hospital, AP-HP, Paris, France

[8]Centre de Référence des Microangiopathies Thrombotiques (CNR-MAT) AP-HP Paris France

Correspondence
Karen Vanhoorelbeke, Laboratory for Thrombosis Research, IRF Life Sciences, KU Leuven Campus Kulak Kortrijk Etienne Sabbelaan 53, B-8500 Kortrijk, Belgium.
Email: karen.vanhoorelbeke@kuleuven.be

Handling Editor: Dr Johnny Mahlangu

Abstract

Background: Thrombotic thrombocytopenic purpura (TTP) is characterized by severe ADAMTS-13 activity deficiency (<10%). Diagnostic testing is challenging because of unavailability, high cost, and expert technician requirement of ADAMTS-13 enzyme assays. Cost-effective, automated fiber-optic surface plasmon resonance (FO-SPR) platforms show potential for developing diagnostic tests. Yet, FO-SPR has never been explored to measure enzymatic activities.

Objectives: To develop an easy-to-use ADAMTS-13 activity assay utilizing optical fibers to rapidly diagnose TTP.

Methods: The ADAMTS-13 activity assay was designed and optimized using FO-SPR technology based on a previously described enzyme-linked immunosorbent assay setup. A calibration curve was generated to quantify ADAMTS-13 activity in plasma of healthy donors and patients with acute immune-mediated TTP (iTTP), hemolytic uremic syndrome, or sepsis. ADAMTS-13 activity data from FO-SPR and fluorescence resonance energy transfer-based strategies (FRETS)-VWF73 reference assays were compared.

Results: After initial assay development, optimization improved read-out magnitude and signal-to-noise ratio and reduced variation. Further characterization demonstrated a detection limit (6.8%) and inter-assay variation (Coefficient of variation, 7.2%) that showed good analytical sensitivity and repeatability. From diverse plasma samples, only plasma from patients with acute iTTP showed ADAMTS-13 activities below 10%. Strong Pearson correlation ($r = 0.854$) between FO-SPR and reference FRETS-VWF73 assays were observed for all measured samples.

Conclusions: A fast ADAMTS-13 activity assay was designed onto automated FO-SPR technology. Optimization resulted in sensitive ADAMTS-13 activity measurements with a detection limit enabling clinical diagnosis of TTP within 3 hours. The FO-SPR assay proved strong correlation with the reference FRETS-VWF73 assay. For the first time,

this assay demonstrated the capacity of FO-SPR technology to measure enzymatic activity in pre-clinical context.

KEYWORDS
ADAMTS-13 protein, diagnostic testing, enzyme assays, optical fibers, purpura, thrombotic thrombocytopenic

Essentials

- Easy-to-use ADAMTS-13 enzyme assays support thrombotic thrombocytopenic purpura diagnosis.
- Fiber-optic surface plasmon resonance shows potency for easy-to-use diagnostic testing.
- A new, fast ADAMTS-13 activity assay was designed and optimized on an automated fiber-optic surface plasmon resonance platform.
- Patients' plasma analysis verified thrombotic thrombocytopenic purpura diagnosis with strong correlation to fluorescence resonance energy transfer-based strategies reference assay.

1 | INTRODUCTION

Thrombotic thrombocytopenic purpura (TTP) is a rare, but devastating, thrombotic disease caused by a severe deficiency in ADAMTS-13 protease. ADAMTS-13 deficiency results in the accumulation of ultra-large von Willebrand factor (VWF) multimers, which spontaneously bind platelets. The resulting microthrombi obstruct the microvasculature, leading to thrombocytopenia, microangiopathic hemolytic anemia, and ischemic organ damage (eg, kidneys, brain, heart) in patients with TTP [1,2]. These clinical signs and symptoms overlap with other thrombotic microangiopathies (TMAs), like hemolytic uremic syndrome (HUS) [2–4]. To prevent misdiagnosis and initiate appropriate treatment in time, distinction between TTP and alternative TMAs within 4 to 8 hours of patient presentation is crucial [5–7]. To date, TTP diagnosis is only confirmed by an ADAMTS-13 activity below 10% (equal to 10 International Units (IU)/dL) of normal ADAMTS-13 activity [1,2,8,9]. Sub-diagnosis can be made based in the presence of inhibitory and/or clearance anti-ADAMTS-13 autoantibodies for immune-mediated TTP (iTTP) or in the absence of anti-ADAMTS-13 autoantibodies together with genetic screening for causative mutations in the *ADAMTS-13* gene for congenital TTP [1,2]. Treatment is aimed at restoring ADAMTS-13 activity levels, although ADAMTS-13 activity remains low in some patients despite clinical remission, which underlines the need for long-term ADAMTS-13 activity follow-up in the management of patients with TTP. Most commonly used assays to measure ADAMTS-13 activity include gold standard fluorescence resonance energy transfer-based strategies (FRETS) [10,11] and in-house or commercial enzyme-linked immunosorbent assay-based assays [12,13]. However, both types of enzyme assays are considered complex and laborious, requiring well-trained laboratory technicians, which restricts their availability to highly expert laboratories. When patients are hospitalized in non-expert centers, sample shipping for ADAMTS13 evaluation can delay the diagnostic consolidation up to 5 days, slowing down the initiation of appropriate treatment. Hence, fast and automated tools for the

analysis of ADAMTS-13 activity, that are cost-effective and easy-to-use, are required for efficient diagnosis and long-term follow-up of patients with TTP admitted in expert or non-expert TTP centers [1,2,14]. Although over the last decade, rapid or automated diagnostic testing to determine ADAMTS-13 activity became available by means of the Ceveron s100 [15,16] and AcuStar [17] instruments. However, there is still room for novel, automated enzyme assays. Indeed, to date, such automated instruments are used by only 25% to 30% of the participants in an *External quality Control for Assays and Tests ADAMTS-13 survey*, highlighting the unavailability of automated diagnostic testing [18]. As an alternative, fiber-optic surface plasmon resonance (FO-SPR) technology could be used to design an ADAMTS-13 activity assay, as this platform allows the development of fast and automated diagnostic assays. FO-SPR has initially been developed as a robust and easy-to-use platform that overcomes many of the limitations of classical surface plasmon resonance systems (eg, Biacore SPR systems). Available as a small benchtop device using inexpensive, disposable dip-in optical fibers, FO-SPR technology has been successfully used to evaluate DNA [19–21] and protein–protein interactions [22,23]. Diagnostic FO-SPR-based assays with single sample testing have been described for sensitive monitoring of patient antibodies in complex matrices such as whole blood and serum. Such examples include measurement of infliximab, adalimumab, and anti-receptor binding domain antibodies in patients with inflammatory bowel disease, including Crohn's disease, and COVID-19, respectively [24–27]. As an innovative technology, FO-SPR platforms have found their way to a broad range of applications for fundamental and diagnostic research purposes. Remarkably, FO-SPR technology has not been explored in the context of enzymatic activity evaluation to the best of our knowledge. Therefore, this study aimed to develop an FO-SPR assay to determine the enzymatic activity of ADAMTS-13. Since such an automated FO-SPR assay would be fast, cost-effective, easy-to-use, and require minimal sample preparation, it would help to answer this unmet clinical need in TTP diagnosis in every routine clinical laboratory.

2 | MATERIALS AND METHODS

2.1 | Healthy donor and patient plasma samples

Citrated plasma was available from 8 healthy donors (KU Leuven, Belgium), 8 patients with acute iTTP (C2VN, Marseille, France), 8 patients having sepsis with known *Staphylococcus aureus* bacteremia before treatment (UZ Leuven, Leuven, Belgium), and 8 patients with HUS from the *French Reference Center for Thrombotic Microangiopathies* (AP-HP, Paris, France). By pooling plasma of over 20 healthy donors, normal human plasma (NHP) was generated. The study was approved by the Ethical Committees of KU Leuven, Belgium (S66725); the Projet National de Recherche clinique 2007, Marseille, France (N°#2007/23); UZ Leuven, Belgium (NCT0191162), Hôpital Pitié-Salpêtrière, Hôpital Saint-Antoine, and Hôpital Lariboisière, Paris, France (NCT00426686), and informed consent was obtained in accordance with the Declaration of Helsinki. All samples were stored at −80 °C, thawed for 5 minutes at 37 °C and vortexed use.
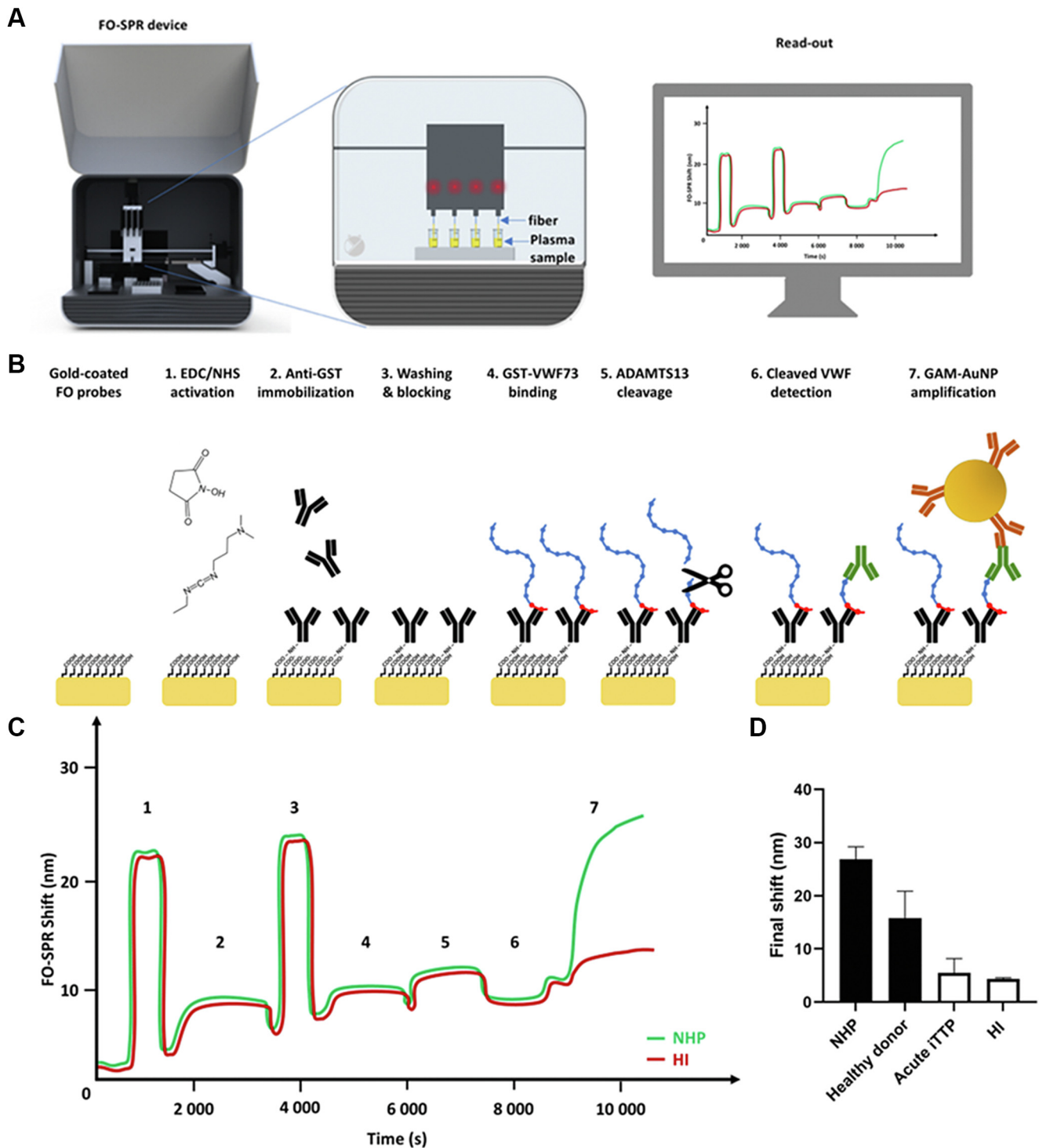
2.2 | FRETS ADAMTS-13 activity assay

An in-house FRETS-VWF73 assay [10,28] was used to measure ADAMTS-13 activity in the plasma samples of healthy donors and patients with acute iTTP, HUS, or sepsis. Enzymatic activity was assessed by mixing plasma, containing ADAMTS-13, with a constant amount of fluorogenic FRETS-VWF73 substrate (2 μM final concentration, PeptaNova GmbH) in HEPES (4-(2-hydroxyethyl)-1-piperazineethanesulfonic acid) buffered saline (50 mM HEPES, 1 μM $ZnCl_2$, 5 mM $CaCl_2.2H_2O$, and 150 mM NaCl) with 1 mg/mL bovine serum albumin in a 96-well White Lia plate (Greiner Bio-One, Vilvoorde, Belgium) with final volume of 200 μL. The plate was incubated at 37°C and fluorescence intensity was detected for 30 cycles of 2.5 minutes using a FLUOstar Optima reader (BMG Labtech GmbH) at 340 nm excitation and 450 nm emission wavelengths [28]. Detected fluorescence signal is directly proportional to the cleavage of FRETS-VWF73 substrate by ADAMTS-13 and was plotted as a function of time with the slopes of the linear part indicating the proteolysis rate [10]. A reference curve was obtained from the slopes of different NHP dilutions (0.5, 0.75, 1, 1.25, 1.5, 1.75, 2% v/v), allowing the estimation of relative ADAMTS-13 activity using ADAMTS-13 activity in NHP as 100%. As negative control conditions, 2% v/v NHP in presence of 10 mM of EDTA or 10 μg/mL of inhibitory anti-ADAMTS-13 antibody 3H9 was evaluated [29,30]. Samples of healthy donors, patients with sepsis, and patients with HUS were assessed using 1.25% v/v plasma, whereas samples from patients with acute iTTP were analyzed using 2.5% v/v plasma.

2.3 | FO-SPR ADAMTS-13 activity assay

The FO-SPR technology uses dip-in optical fibers (FO probes, FOx Biosystems) on the automated White FOx 1.0 platform (FOx

Biosystems). Using FOx software (FOx Biosystems), the robotic arm of the FO-SPR platform guides the FO probes into all dip-in solutions and FO probe agitation (0-2000 rpm) is programmed for several binding steps. Also, FOx software records and visualizes real-time changes in the refractive index, measured as a nm shift, corresponding to analyte binding to antibodies present on gold-coated FO probes (Figure 1A). The setup of the FO-SPR ADAMTS-13 activity assay was based on the immunoassay described by Kato et al. [12] (Figure 1A) that shows a graphical representation of the FO-SPR device, together with a close-up of FO probes dipped in plasma samples giving a real-time FO-SPR shift. The individual immersion steps, always requiring 150 μL dip-in solution, are shown in (Figure 1B). First, the carboxyl self-assembly monolayer (SAM) present on the optical fibers was chemically activated (Figure 1B; step 1) by dipping FO probes in a 400/100 mM 1-ethyl-3-[3-dimethylaminopropyl] carbodiimide/N-hydroxysuccinimide solution in 50 mM MES hydrate (2-(N-Morpholino)ethanesulfonic acid hydrate) buffer for 5 minutes. Next, the probes were submersed into a polyclonal goat anti-glutathione S-transferase (GST) antibody solution (in 10 mM sodium acetate (NaAc) buffer, Rockland) for 30 minutes at 400 rpm which allowed covalent coupling of the anti-GST antibody amino group to the carboxyl SAM of the optical fiber (Figure 1B; step 2). The nm shift accompanied with binding of the anti-GST antibodies is referred to as the immobilization shift. Unbound antibody was removed by dipping the FO probes twice in 10 mM glycine regeneration buffer (pH 2) for 30 seconds, after which the remaining free SAM carboxyl groups were blocked by dipping the FO probe for 8 minutes in SuperBlock buffer (ThermoFisher Scientific) to prevent undesired protein interactions with the FO probes (Figure 1B; step 3). Next, the FO probes were dipped into a solution containing GST-tagged VWF73 substrate (produced and purified as previously described for murine GST-VWF73 [31]) in phosphate buffered saline containing 0.01% v/v Tween20 for 20 minutes at 400 rpm (Figure 1B; step 4) to allow capturing of GST-tagged VWF73 substrate to the covalently coupled anti-GST antibodies. Next, cleavage of immobilized VWF73 substrate by plasma ADAMTS-13 was initiated by immersing the FO probe in plasma that was 1/11 diluted in piperazine-N,N′-bis(2-ethanesulfonic acid) (PIPES) reaction buffer (10 mM PIPES, 5 mM $MgCl_2.6H_2O$, 5 mM benzamidine hydrochloride hydrate, 1 mM tranexamic acid, pH 6) for 20 minutes at 400 rpm (Figure 1B; step 5). Cleaved GST-tagged VWF73 substrate on the probe was then detected by dipping the probe in a solution containing a monoclonal mouse anti-human VWF-A2 (ADAMTS-13-cleaved) antibody (R&D Systems) in phosphate buffered saline containing 0.01% v/v Tween20 for 20 minutes at 400 rpm. This anti-VWF-A2 antibody specifically binds to the cleaved VWF decapeptide (Asp1596-Tyr1605) (Figure 1B; step 6). Finally, the FO probe was immersed in phosphate buffered saline/0.5% bovine serum albumin containing goat antimouse antibody conjugated 40 nm gold nanoparticles (GAM-AuNPs) at OD 1 (optical density at 530 nm) for 20 minutes at 400 rpm (Figure 1B; step 7). This last step is needed to enhance the final signal: the nm shift accompanied with binding of the GAM-AuNPs which is referred to as the final shift. Figure 1C provides a representative sensorgram of the real-time FO-

FIGURE 1 Schematic design of the proof-of-concept FO-SPR ADAMTS13 activity assay. A) Graphical representation of the FO-SPR small benchtop device with close-up of FO probes dipped into plasma samples with real-time FO-SPR shift display. B) The carboxyl self-assembly monolayer present on the surface of gold-coated FO probes require chemical activation using EDC/NHS chemistry (step 1) to immobilize the anti-GST antibody onto the FO probe (step 2). After unbound antibody removal and blocking (step 3), the GST-tagged VWF73 substrate is bound (step 4). Next, the FO probe is dipped into plasma containing ADAMTS13 to cleave VWF73 (step 5) followed by antibody detection of only the cleaved substrate (step 6). Signal amplification using goat anti-mouse conjugated gold nanoparticles (step 7), generates the final FO-SPR shift. C) Sensorgram displaying the typical, real-time FO-SPR shifts of the ADAMTS13 activity assay on a dip-in FO probe when analyzing NHP or HI plasma. D) Proof-of-concept measurement discriminating final shifts from plasma samples rich (NHP & healthy donor, filled bars) and poor (acute iTTP & HI plasma, unfilled bars) in ADAMTS13 activity. Data is presented as mean with one standard deviation. FO-SPR, fiber-optic surface plasmon resonance; GAM-AuNP, goat anti-mouse conjugated gold nanoparticle; HI, heat inactivated plasma; NHP, normal human plasma; iTTP, immune-mediated thrombotic thrombocytopenic purpura.

SPR read-out (shift in nm) for both NHP and heat-inactivated (HI; NHP plasma incubated for 1 hour at 56 °C and spun down at 9600 × g) plasma. This default protocol was programmed into the FOx software, allowing all FO probe immersion steps to occur fully automated.

2.4 | Optimization of the different steps in the FO-SPR ADAMTS-13 activity assay

To further optimize the FO-SPR ADAMTS-13 activity assay, steps 2, 4, and 6 (Figure 1B) of this FO-SPR assay were evaluated in more detail. To covalently immobilize the polyclonal goat anti-GST antibody (step 2), different antibody concentrations (20, 10, and 5 μg/mL) and NaAc buffers with different pH (pH 5, 6, and 7) were assessed. Also, the effects of several concentrations of the GST-tagged VWF73 substrate (1, 0.5, 0.1 μg/mL) (step 4) and the monoclonal mouse antihuman vWF-A2 (ADAMTS-13-cleaved) detection antibody (5, 1, 0.1 μg/mL) (step 6) on the final shift were determined.

2.5 | Setting up a calibration curve and measuring plasma samples using the optimized FO-SPR ADAMTS-13 activity assay

When setting up a calibration curve for the FO-SPR ADAMTS-13 activity assay, a 1/11 dilution of NHP in PIPES reaction buffer was set as 100% ADAMTS-13 activity. For each data point (n = 3) of the ADAMTS-13 activity calibration curve, the 1/11 NHP dilution was additionally diluted (1/2, 1/2.5, 1/3.33, 1/5, 1/6.66, 1/10, and 1/20) with HI plasma to adjust plasma ADAMTS-13 activities and maintain a constant plasma matrix. As for the negative control conditions, 10 mM EDTA or 10 μg/mL inhibitory anti-ADAMTS-13 antibody 3H9 was added to NHP plasma. When evaluating ADAMTS-13 activity of healthy donors or patients with acute iTTP, HUS, and sepsis, plasma samples were additionally mixed (respectively 1/5, undiluted, 1/3.33 and 1/2) with HI plasma while maintaining the final 1/11 plasma dilution.

2.6 | Statistical analysis

GraphPad Prism v9.0.0 statistical software (GraphPad Software) was used to test Shapiro–Wilk normality, one-way analysis of variance with multiple comparison using Tukey's correction, Pearson r correlation coefficient, simple linear regression, and for Bland-Altman analysis during statistical analysis of the assay optimization, characterization, and validation. All data are presented as mean ± one SD. A P value of <.05 was considered statistically significant.

3 | RESULTS

3.1 | Initial proof-of-concept of FO-SPR-based measurement of ADAMTS-13 enzymatic activity

Based on previous expertise, we first used an initial assay setup (in detail described in the method section) to determine ADAMTS-13 activity in plasma. As depicted in Figure 1B, optical fibers required 1-ethyl-3-[3-dimethylaminopropyl] carbodiimide/N-hydroxysuccinimide chemical activation of the carboxyl groups of the SAM (step 1). Afterward, the initial setup included 20 μg/mL anti-GST antibody (in 10 mM NaAc buffer at pH 5) immobilization (step 2), FO probe washing and blocking (step 3), and binding of GST-tagged VWF73 substrate (1 μg/mL, step 4). Bound VWF73 substrate was cleaved by plasma ADAMTS-13 (1/11 diluted, step 5) and detected using monoclonal mouse antihuman VWF-A2 (ADAMTS-13-cleaved) antibody (5 μg/mL, step 6). Signal amplification was done using GAM-AuNPs (step 7). Samples used in initial proof-of-concept experiments included NHP, healthy donor plasma, acute iTTP plasma and HI plasma. Interestingly, using this first assay setup, the FO-SPR assay gave a specific and quantitative final shift for ADAMTS-13 activity (Figure 1D). Indeed, this assay resulted in high final shifts reflecting high ADAMTS-13 activity in NHP (26.8 nm ± 2.4 nm; 8.8% CV, coefficient of variation percentage) and healthy donor (15.8 nm ± 5.1 nm; 32.1% CV) plasma but not in patients with acute iTTP (5.5 nm ± 2.7 nm; 48.4% CV) and HI plasma (4.4 nm ± 0.2 nm; 4.7% CV) (Figure 1D). However, large standard deviations with corresponding high % CVs prompted us to further optimize the different binding steps of this FO-SPR ADAMTS-13 activity assay.

3.2 | Optimization of assay steps to measure ADAMTS-13 activity via FO-SPR

To improve inter-assay repeatability and sensitivity of the ADAMTS-13 activity assay, the binding steps of the anti-GST antibody (Figure 1B; step 2), the GST-tagged VWF73 substrate (Figure 1B; step 4) and the antihuman VWF-A2 (ADAMTS-13-cleaved) detection antibody (Figure 1B; step 6) were optimized. By measuring both NHP and HI plasma, the effect of different buffer compositions, buffer pHs, and antibody concentrations on the immobilization or final FO-SPR shift were studied. Preferential binding conditions were selected based on the magnitude of the immobilization or final FO-SPR shift, the SD, the % CV of repeated measurements, and on the NHP/HI plasma signal-to-noise ratio of the final shift. First, by evaluating the immobilization shift, the efficiency of the anti-GST antibody immobilization onto the FO probe was measured by varying both the antibody concentration (20, 10, 5 μg/mL) and NaAc buffer pH values (pH 5, 6, 7) (Figure 2A). No statistical differences in the immobilization shifts were observed among different antibody concentrations. In contrast, the NaAc buffer pH largely impacted the immobilization
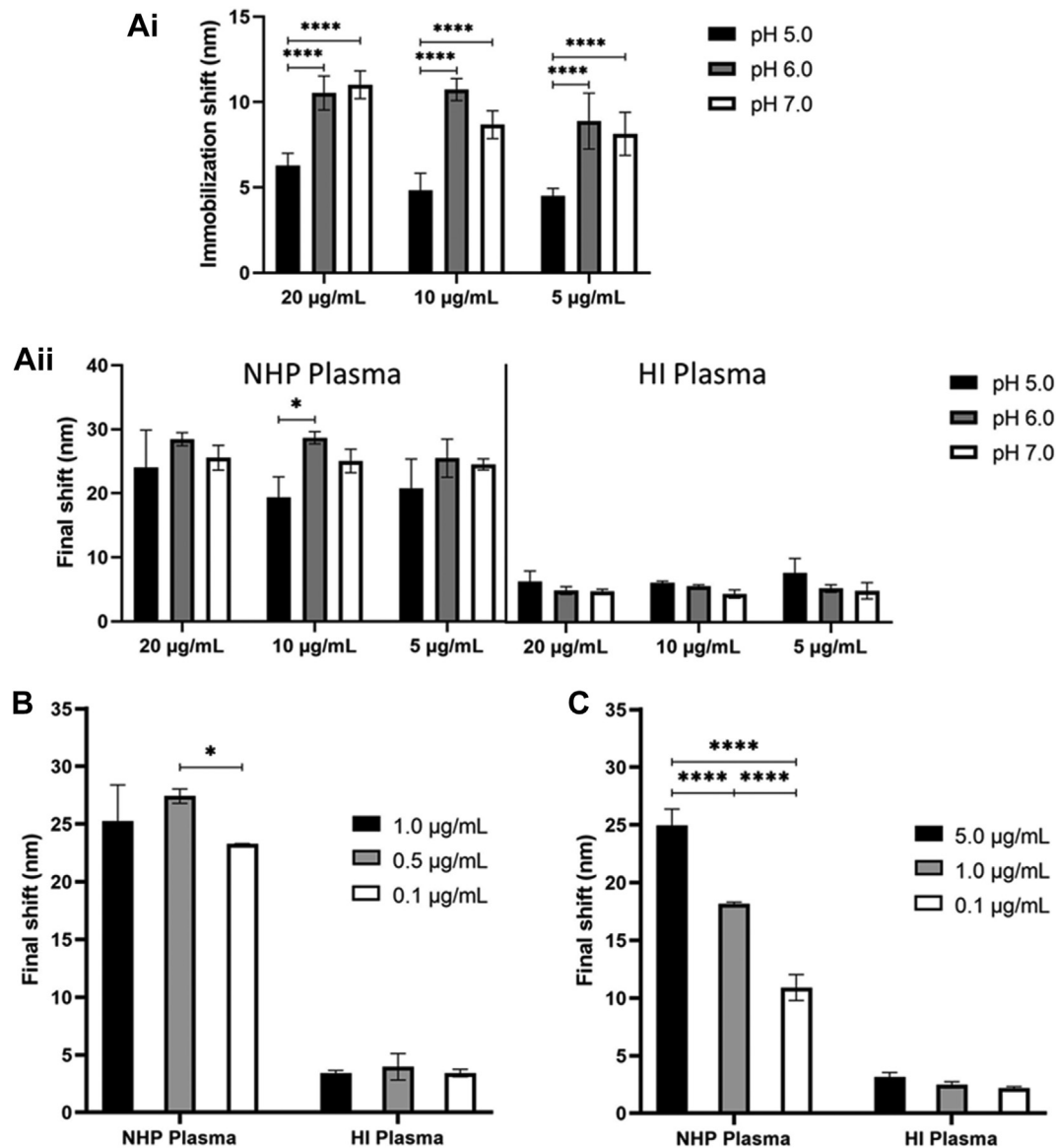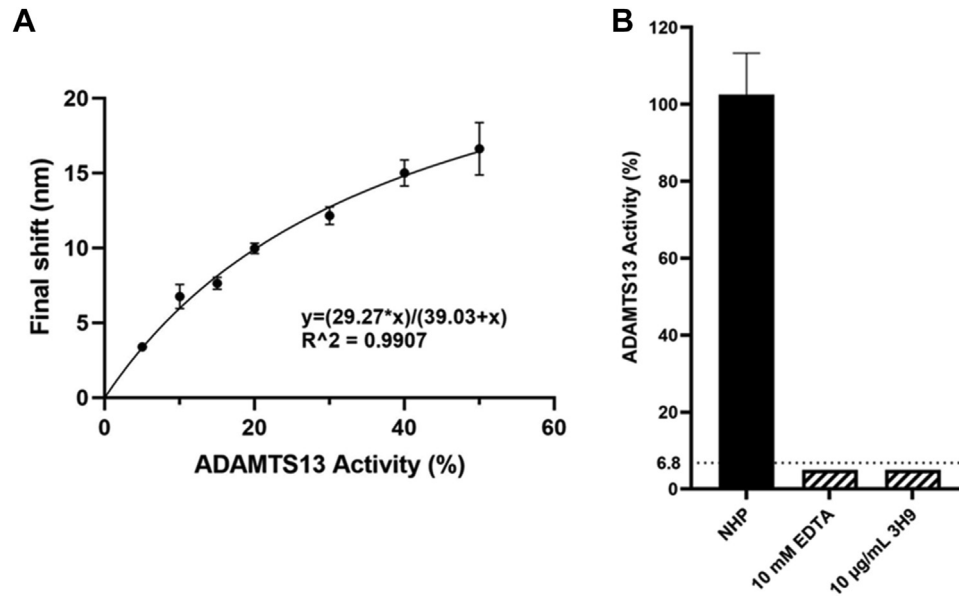
FIGURE 2 FO-SPR ADAMTS13 activity assay optimization. Ai) Effect of the anti-GST antibody concentration and sodium acetate buffer pH on the antibody immobilization efficiency onto the FO probes (n = 6). Aii) Effect of the anti-GST antibody concentration and sodium acetate buffer pH on the magnitude of the final shift after signal amplification when assessing NHP (n = 3) and HI (n = 3) plasma. B) Evaluation of the effect of various GST-tagged VWF73 substrate concentrations on the magnitude of the final shift in NHP (n = 3) and HI (n = 3) plasma. C) Effect of different anti-VWF detection antibody concentrations on the final shift in NHP (n = 3) and HI (n = 3) plasma. Data represents mean with one standard deviation, statistically significant difference is indicated using an asterisk (*) when $P < .05$. HI, heat inactivated plasma; NHP, normal human plasma.

efficiency as this was significantly higher at pH 6 and pH 7 compared with pH 5 ($P < .0001$). These results suggest higher immobilization efficiencies at higher pH values. When evaluating the final shift, the higher antibody immobilization efficiency at pH 6 and pH 7 was minimally reflected (Figure 2A). Yet, the condition using 10 µg/mL anti-GST antibody showed significantly higher final shifts when using NaAc buffer of pH 6 compared with pH 5 ($P = .0308$). This condition gave the highest immobilization and final shifts for NHP plasma and showed the lowest SD and % CV. As expected for measuring HI plasma, background signals remained equally low when using different immobilization conditions, which suggests low variation and high

NHP/HI plasma signal-to-noise ratios. Therefore, this immobilization condition (10 µg/mL anti-GST antibody in NaAc buffer of pH 6) was chosen for all further experiments.

Using the selected immobilization condition, the effect of the GST-tagged VWF73 substrate concentration bound to the immobilized anti-GST antibody (Figure 1B; step 4) was evaluated. Various concentrations (1, 0.5, 0.1 µg/mL) were used and final shifts were assessed. As shown in Figure 2B, the final shifts when measuring ADAMTS-13 activity in NHP were highest for the 0.5 µg/mL condition, only reaching statistical significance compared with the 0.1 µg/mL condition ($P = .0303$). As the final shift for all HI plasma conditions

A

$$y=(29.27^*x)/(39.03+x)$$
$$R^2 = 0.9907$$

B

FIGURE 3 Calibration curve of the FO-SPR ADAMTS13 activity assay and negative controls. A) Non-linear regression calibration curve of plasma ADAMTS13 activity: $y = (29.27^*x)/(39.03+x)$; $R^2 = 0.9907$. Error bars represent one standard deviation (n = 3). B) As a negative control, NHP plasma was preincubated with 10 mM EDTA or 10 µg/mL of the inhibitory anti-ADAMTS13 mAb 3H9 which abolished ADAMTS13 activity as shown by the undetectable ADAMTS13 activity (below the FO-SPR assay detection limit of 6.8%, dotted line). Error bar represents standard deviation (n = 3). EDTA, ethylenediaminetetraacetic acid; NHP, normal human plasma.

showed low signals, similar NHP/HI plasma signal-to-noise ratios were observed for all substrate concentrations. The condition using 0.1 µg/mL GST-tagged VWF73 substrate resulted in the lowest SD and % CV, which was therefore selected for all further experiments. Finally, the effect of different antihuman VWF-A2 (ADAMTS-13-cleaved) antibody concentrations (5, 1, 0.1 µg/mL) (Figure 1B; step 6) on the final shift was evaluated. Using NHP plasma, a strong dose-response was observed for the antihuman VWF-A2 (ADAMTS-13-cleaved) antibody concentration and the final shift. As expected, different detection antibody concentrations did not affect the low final shifts observed for HI plasma. The condition using the highest antibody concentration (5 µg/mL) was selected for further experiments, as it showed the highest final shift and highest NHP/HI plasma signal-to-noise ratio with a good SD and % CV below 10% (Figure 2C).

Taken together, after optimizing crucial binding steps in the setup, we defined the fully optimized FO-SPR ADAMTS-13 activity assay as the one using 10 µg/mL anti-GST immobilization antibody coupled at pH 6, 0.1 µg/mL GST-tagged VWF73 substrate, and 5 µg/mL antihuman vWF-A2 (ADAMTS-13-cleaved) detection antibody. These conditions allowed to reproducibly discriminate plasma samples with high or low final shift (reflecting ADAMTS-13 activity) with limited variation.

triplicate. All data points used a fixed 1/11 plasma dilution, with 1/11 diluted NHP set as the 100% ADAMTS-13 activity reference. Calibration data points were obtained by additionally diluting NHP with HI plasma to enable plasma sample preparation with variable ADAMTS-13 activity (50%, 40%, 30%, 20%, 15%, 10%, and 5%) while maintaining constant plasma matrix conditions (ie, 1/11 diluted plasma). A non-linear regression, one-site specific binding calibration curve (y = 29.27*x/(39.03+x); $R^2 = 0.9907$) was generated with the x-axis representing plasma ADAMTS-13 activity and y-axis the final shift (in nm). In Figure 3A, the average final shifts for the plasma ADAMTS-13 activity were plotted with corresponding standard deviations. All individual data points showed a % CV below 12.5%, and the mean inter-assay % CV was 7.2%. Also, the limit of detection (LoD, LoD = 29.27*(x(0)+3σ) / (39.03+(x(0)+3σ))) and lower limit of quantification (LLoQ, LLoQ = 29.27*(x(0)+10σ) / (39.03+(x(0)+10σ))) for ADAMTS-13 activity were calculated from repeated measurements using HI plasma (n = 9) and equaled 6.8% and 11.3%, respectively. Additional negative control conditions included incubation of NHP plasma with 10 mM EDTA or 10 µg/mL inhibitory anti-ADAMTS-13 antibody 3H9 to overrule plasma ADAMTS-13 activity. As presented in Figure 3B, undetectable ADAMTS-13 activity levels (ie, below the 6.8% detection limit) were observed.

3.3 | FO-SPR ADAMTS-13 activity quantification

To further characterize the potential of the FO-SPR ADAMTS-13 activity assay for TTP diagnosis, we used the optimized FO-SPR ADAMTS-13 activity assay to generate a calibration curve in

3.4 | FO-SPR ADAMTS-13 activity assay for the diagnosis of TTP

To validate the diagnostic testing potential of the FO-SPR ADAMTS-13 activity assay, 8 plasma samples from healthy donors, 8 plasma
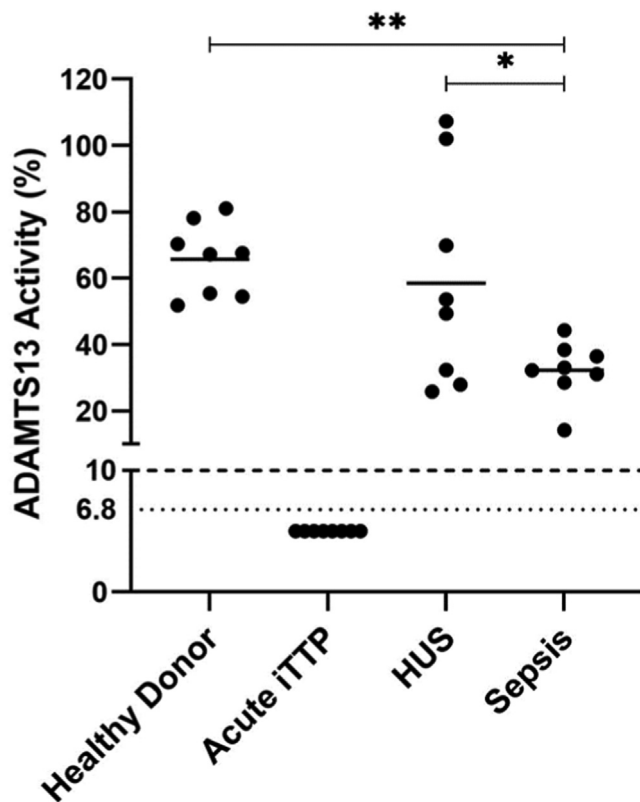
FIGURE 4 Diagnostic validation of the FO-SPR ADAMTS13 activity assay. Evaluation of ADAMTS13 activity levels in 8 plasma samples of healthy donors, acute iTTP patients, HUS patients or sepsis patients with known Staphylococcus aureus bacteremia before treatment. For each sample type, mean ADAMTS13 activity with error bars representing standard deviation, is shown. Statistical significant differences are indicated with an asterisk (*) when $P < .05$. Dotted line represents the detection limit (6.8%) of the FO-SPR ADAMTS13 activity assay, whereas the striped line indicates the ADAMTS13 activity diagnostic cut-off value (10%) for TTP disease. HUS, hemolytic uremic syndrome; iTTP, immune-mediated thrombotic thrombocytopenic purpura.

samples from patients with acute iTTP, and 8 plasma samples from patients with HUS were screened. As an additional reference, 8 samples from patients with sepsis were tested, as these patients are known to have decreased ADAMTS-13 activity levels, although typically not <10% [4,32]. ADAMTS-13 activity levels measured from healthy donor plasma ranged between 52% and 81% (mean = 66%), which fits the reported ranges for healthy individuals [4,33]. All acute iTTP patient samples showed an ADAMTS-13 activity below the 6.8% LoD, confirming their diagnosis of acute iTTP with an ADAMTS-13 activity below the diagnostic cut-off of 10% (Figure 4; Supplementary Table S1). ADAMTS-13 activities ranged between 26% and 107% for patients with HUS (mean = 59%) and between 14% and 44% for patients with sepsis (mean = 32%). Hence, the fully optimized and characterized FO-SPR ADAMTS-13 activity assay allows to diagnose patients with acute iTTP and could successfully discriminate acute iTTP from HUS (another TMA) and from sepsis.
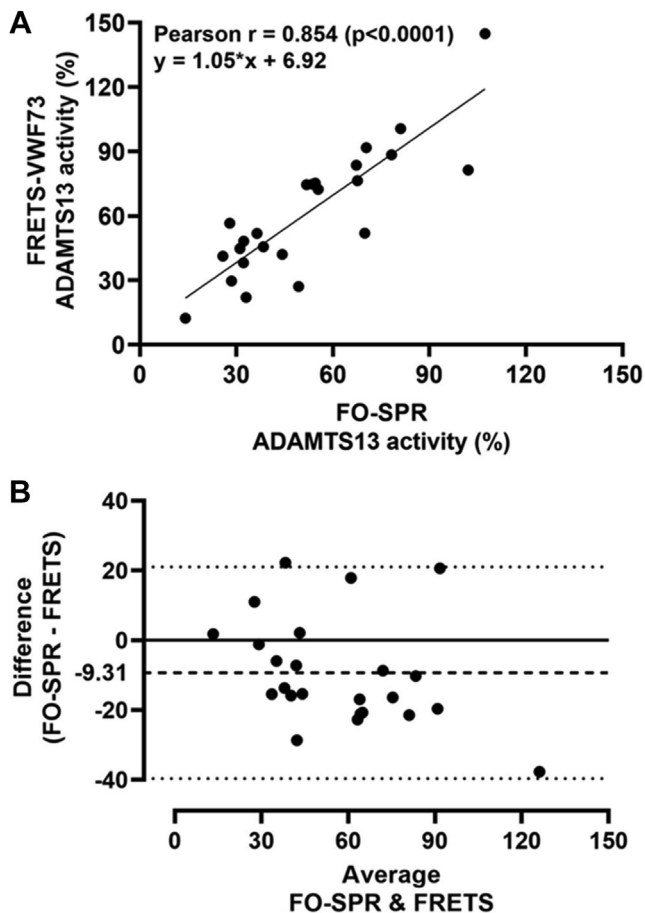
3.5 | FO-SPR vs FRETS comparative analysis

Finally, we compared quantitative results from the FO-SPR ADAMTS-13 activity assay with those measured via the FRETS-VWF73 assay, a reference assay in many research and clinical laboratories [10,11]. ADAMTS-13 activity of all healthy donors, and patients with acute iTTP, HUS, and sepsis were evaluated in our in-house FRETS-VWF73 assay (Supplementary Table S1). Compared with the FO-SPR assay, similar ranges were found for the ADAMTS-13 activity levels in healthy donor (72%-101%, mean = 83%), HUS (27%-145%, mean 66%), and sepsis (12%-52%, mean = 36%) plasma samples. Similarly, patients with acute iTTP showed undetectable ADAMTS-13 activity (<10%) when evaluated using the FRETS-VWF73 assay. Strong Pearson r correlation ($r = 0.854$; $P < .0001$; $y = 1.05*x + 6.92$) was observed between ADAMTS-13 activity determined by FO-SPR and FRETS-VWF73 assays (Figure 5A). As reflected by the 95% confidence intervals (95% CI) of the slope (95% CI: 0.7646-1.327) and the y-intercept (95% CI: −9.209 to 23.05), no statistically significant proportional (95% CI of the slope encloses 1) and systematic bias (95% CI of the y-intercept encloses 0) were observed. To visualize the behavior of the differences between both methods, Bland-Altman analysis was performed (Figure 5B) [34]. Similarly, no significant systematic bias was observed (zero equality line fits the 95% CI of the mean bias), whereas a small proportional bias (−9.31%) was identified when measuring plasma samples with ADAMTS-13 activity above 50%.

4 | DISCUSSION

For optimal prognosis of patients with TTP, correct diagnosis and subsequent treatment initiation within 4 to 8 hours after admission is crucial [5–7]. To date, ADAMTS-13 enzyme assays, typically including FRETS- and enzyme-linked immunosorbent assay-based assays, are only available in highly expert laboratories as diagnostic testing remains time-consuming, laborious, and require well-trained staff. When patients are hospitalized at non-reference centers, patient samples need to be shipped, delaying the diagnostic consolidation up to 5 days. Currently, automated instruments, such as the HemosIL AcuStar and Ceveron s100, are still limitedly present in routine clinical laboratories and discrepant lower ADAMTS-13 activity levels were reported when using the HemosIL AcuStar instrument resulting in false positive TTP diagnosis of alternative patients with TMA [15]. The rapid Technoscreen assay is also available but is, however, semi-quantitative and potentially less useful to diagnose TTP [35]. To try to answer the unmet needs of clinical ADAMTS-13 testing for the diagnosis of patients with TTP, this study aimed at developing a fast, easy-to-use diagnostic assay using automated, cost-effective FO-SPR technology to measure ADAMTS-13 activity in real-time. The FO-SPR ADAMTS-13 activity assay was characterized by a non-linear calibration curve, an inter-assay variation of 7.2%, and LoD and LLoQ of 6.8% and 11.3%, respectively. Given this analytical sensitivity, plasma samples from healthy donors and patients with acute iTTP, HUS, and sepsis

FIGURE 5 Comparative analysis of FO-SPR and FRETS ADAMTS13 activity assays. A) Pearson *r* correlation testing of ADAMTS13 activities measured using both FO-SPR and reference FRETS-VWF73 methods showed strong statistically significant correlation (*r* = 0.854, *P* < .0001) and simple linear regression (y = 1.05*x + 6.92) indicated positive correlation. B) Bland-Altman analysis estimates the agreement between both quantitative methods by constructing the 95% limits of agreements (39.66-21.03, dotted lines) and calculates the mean bias (−9.31, striped line) of the FO-SPR ADAMTS13 activity assay compared with the FRETS-VWF73 reference method.

were validated to illustrate the diagnostic potential of the FO-SPR ADAMTS-13 enzyme assay to discriminate patients with acute iTTP from patients with alternative TMA (HUS) or sepsis. Similar ranges for ADAMTS-13 activity were observed and strong Pearson r correlation (*r* = 0.854) was defined when comparing ADAMTS-13 activity determined by both FO-SPR and reference FRETS-VWF73 assays. Bland-Altman analysis illustrated good agreement and no systematic bias between ADAMTS-13 activity measurements by FO-SPR and FRETS-VWF73 methods. A small proportional bias was identified, suggesting lower FO-SPR ADAMTS-13 activity measurements for plasma samples with ADAMTS-13 activity above 50%, hence not affecting the diagnostic potential to discriminate TTP disease from other TMA or sepsis.

Interestingly, FO-SPR technology comes as a small benchtop device that could easily be setup in routine clinical laboratories. Automated FO-SPR technology is easy-to-use, which reduces the handling complexity and restricts staff training required to perform ADAMTS13 testing. After minimal sample preparation, technicians only have to start the default software protocol. The robotic arm is programmed to automatically pick up and direct the disposable, dip-in optical fibers, which allows crude sample processing without cleaning or any risk of system clogging. In future, pre-functionalization of the FO probes and direct detection antibody labeling toward gold nanoparticles could further reduce the assay time, whereas regeneration strategies [23] will allow the use of reusable FO probes to further lower the assay cost. Further validation of the FO-SPR ADAMTS-13 activity assay should include TTP remission samples and samples from patients with relapse, whereas mixing studies would allow the validation of plasma inhibitor presence. Despite being described in a broad range of applications, such as patient (auto)antibody [22,24–27] or hormone [36] detection and as well as in real-time polymerase chain reaction applications [19–21], to the best of our knowledge, this article is the first to report the use of FO-SPR technology in the context of enzymatic activity measurements. As a consequence, FO-SPR technology could be exploited to commercialize diagnostic assays for a broader range of diseases (eg, von Willebrand disease), as well as to expand its relevance in fundamental research on protein interactions and conformations.

In conclusion, our easy-to-use ADAMTS-13 activity assay using the automated and cost-effective FO-SPR technology proves great potential to diagnose TTP disease within 3 hours. Introducing this fast, on-demand ADAMTS-13 enzyme assay into more (non-expert) hospital laboratories could largely improve TTP diagnosis and patient management, whereas the cost-savings and ease-of-use of our FO-SPR ADAMTS-13 activity assay could still benefit expert centers.

AUTHOR CONTRIBUTIONS

Q. Bonnez designed the assay setup and protocol, performed experiments, analyzed data and wrote the manuscript. C. Dekimpe performed experiments and discussed data. E. Tellier, G. Kaplanski, P. Verhamme, B. Joly, P. Coppo, and A. Veyradier provided clinical samples, discussed the data and provided valuable input. C. Tersteeg, S.F. De Meyer, and J. Lammertyn discussed the data, provided valuable input and edited the manuscript. K. Vanhoorelbeke supervised, designed experiments, analyzed data, and wrote the manuscript. All authors discussed results, supplied critical feedback and approved the final version of the manuscript.

RELATIONSHIP DISCLOSURE

A. Veyradier is a member of the French Advisory board for caplaci-zumab (SANOFI) and for recombinant human ADAMTS-13 (TAKEDA). J. Lammertyn is a member of the Board of Directors of FOx Bio-systems. P. Coppo is a member of the advisory board of Sanofi, Alexion, Takeda and Janssen Pharmaceutica. All other authors lack any conflicts of interest.

TWITTER

Quintijn Bonnez 🐦 @BonnezQuintijn
Karen Vanhoorelbeke 🐦 @kvhoorel

REFERENCES

[1] Kremer Hovinga JA, Coppo P, Lämmle B, Moake JL, Miyata T, Vanhoorelbeke K. Thrombotic thrombocytopenic purpura. *Nat Rev Dis Primers.* 2017;3:17020.

[2] Joly BS, Coppo P, Veyradier A. Thrombotic thrombocytopenic purpura. *Blood.* 2017;129:2836–46.

[3] Zheng XL, Vesely SK, Cataland SR, Coppo P, Geldziler B, Iorio A, et al. ISTH guidelines for the diagnosis of thrombotic thrombocytopenic purpura. *J Thromb Haemost.* 2020;18:2486–95.

[4] Roose E, Schelpe AS, Joly BS, Peetermans M, Verhamme P, Voorberg J, et al. An open conformation of ADAMTS-13 is a hallmark of acute acquired thrombotic thrombocytopenic purpura. *J Thromb Haemost.* 2018;16:378–88.

[5] White A, Martin R, Sew K, Stucke A, Cook R. Economic impact of a rapid, on-demand ADAMTS-13 activity assay for the diagnosis of thrombotic thrombocytopenic purpura. *Res Pract Thromb Haemost.* 2022;6:e12711.

[6] Scully M, Hunt BJ, Benjamin S, Liesner R, Rose P, Peyvandi F, et al. Guidelines on the diagnosis and management of thrombotic thrombocytopenic purpura and other thrombotic microangiopathies. *Br J Haematol.* 2012;158:323–35.

[7] Azoulay E, Bauer PR, Mariotte E, Russell L, Knoebl P, Martin-Loeches I, et al. Expert statement on the ICU management of patients with thrombotic thrombocytopenic purpura. *Intensive Care Med.* 2019;45:1518–39.

[8] Furlan M, Robles R, Galbusera M, Remuzzi G, Kyrle PA, Brenner B, et al. von Willebrand factor-cleaving protease in thrombotic thrombocytopenic purpura and the hemolytic-uremic syndrome. *N Engl J Med.* 1998;339:1578–84.

[9] Scully M, Cataland S, Coppo P, de la Rubia J, Friedman KD, Kremer Hovinga J, et al. Consensus on the standardization of terminology in thrombotic thrombocytopenic purpura and related thrombotic microangiopathies. *J Thromb Haemost.* 2017;15:312–22.

[10] Kokame K, Nobe Y, Kokubo Y, Okayama A, Miyata T. FRETS-VWF73, a first fluorogenic substrate for ADAMTS13 assay. *Br J Haematol.* 2005;129:93–100.

[11] Subhan M, Scully M. Advances in the management of TTP. *Blood Rev.* 2022;55:100945.

[12] Kato S, Matsumoto M, Matsuyama T, Isonishi A, Hiura H, Fujimura Y. Novel monoclonal antibody-based enzyme immunoassay for determining plasma levels of ADAMTS13 activity. *Transfusion.* 2006;46:1444–52.

[13] Hubbard AR, Heath AB, Kremer Hovinga JA. Subcommittee on von Willebrand Factor. Establishment of the WHO 1st International Standard ADAMTS13, plasma (12/252): communication from the SSC of the ISTH. *J Thromb Haemost.* 2015;13:1151–3.

[14] Sui J, Zheng L, Zheng XL. ADAMTS13 Biomarkers in management of immune thrombotic thrombocytopenic purpura. *Arch Pathol Lab Med.* 2023;147:974–9.

[15] Singh D, Subhan MO, de Groot R, Vanhoorelbeke K, Zadvydaite A, Dragūnaitė B, et al. ADAMTS13 activity testing: evaluation of commercial platforms for diagnosis and monitoring of thrombotic thrombocytopenic purpura. *Res Pract Thromb Haemost.* 2023;7:100108.

[16] Geiter S, Wagner L, Binder N, Budde U. Evaluation of a new fully automated ADAMTS13 activity assay [abstract]. *Res Pract Thromb Haemost.* 2021;5(Suppl 2).

[17] Favresse J, Lardinois B, Chatelain B, Jacqmin H, Mullier F. Evaluation of the fully automated HemosIL Acustar ADAMTS13 activity assay. *Thromb Haemost.* 2018;118:942–4.

[18] Favaloro EJ, Pasalic L, Henry B, Lippi G. Laboratory testing for ADAMTS13: utility for TTP diagnosis/exclusion and beyond. *Am J Hematol.* 2021;96:1049–55.

[19] Pollet J, Delport F, Janssen KP, Jans K, Maes G, Pfeiffer H, et al. Fiber optic SPR biosensing of DNA hybridization and DNA-protein interactions. *Biosens Bioelectron.* 2009;25:864–9.

[20] Daems D, Pfeifer W, Rutten I, Saccà B, Spasic D, Lammertyn J. Three-dimensional DNA origami as programmable anchoring points for bioreceptors in fiber optic surface plasmon resonance biosensing. *ACS Appl Mater Interfaces.* 2018;10:23539–47.

[21] Daems D, Knez K, Delport F, Spasic D, Lammertyn J. Real-time PCR melting analysis with fiber optic SPR enables multiplex DNA identification of bacteria. *Analyst.* 2016;141:1906–11.

[22] Horta S, Qu JH, Dekimpe C, Bonnez Q, Vandenbulcke A, Tellier E, et al. Co(III)-NTA mediated antigen immobilization on a fiber optic-SPR biosensor for detection of autoantibodies in autoimmune diseases: application in immune-mediated thrombotic thrombocytopenic purpura. *Anal Chem.* 2020;92:13880–7.

[23] Qu JH, Leirs K, Escudero R, Strmšek Z, Jerala R, Spasic D, et al. Novel regeneration approach for creating reusable FO-SPR probes with NTA surface chemistry. *Nanomaterials (Basel, Switzerland).* 2021;11:186.

[24] Lu J, Van Stappen T, Spasic D, Delport F, Vermeire S, Gils A, et al. Fiber optic-SPR platform for fast and sensitive infliximab detection in serum of inflammatory bowel disease patients. *Biosens Bioelectron.* 2016;79:173–9.

[25] Lu J, Spasic D, Delport F, Van Stappen T, Detrez I, Daems D, et al. Immunoassay for detection of infliximab in whole blood using a fiber-optic surface plasmon resonance biosensor. *Anal Chem.* 2017;89:3664–71.

[26] Bian S, Lu J, Delport F, Vermeire S, Spasic D, Lammertyn J, et al. Development and validation of an optical biosensor for rapid monitoring of adalimumab in serum of patients with Crohn's disease. *Drug Test Anal.* 2018;10:592–6.

[27] Qu JH, Leirs K, Maes W, Imbrechts M, Callewaert N, Lagrou K, et al. Innovative FO-SPR label-free strategy for detecting anti-RBD antibodies in COVID-19 patient serum and whole blood. *ACS Sens.* 2022;7:477–87.

[28] Schelpe AS, Orlando C, Ercig B, Geeroms C, Pareyn I, Vandeputte N, et al. Child-onset thrombotic thrombocytopenic purpura caused by p.R498C and p.G259PfsX133 mutations in ADAMTS13. *Eur J Haematol.* 2018:R498C.

[29] Feys HB, Roodt J, Vandeputte N, Pareyn I, Lamprecht S, van Rensburg WJ, et al. Thrombotic thrombocytopenic purpura directly linked with ADAMTS13 inhibition in the baboon (Papio ursinus). *Blood.* 2010;116:2005–10.

[30] Deforche L, Roose E, Vandenbulcke A, Vandeputte N, Feys HB, Springer TA, et al. Linker regions and flexibility around the metalloprotease domain account for conformational activation of ADAMTS-13. *J Thromb Haemost.* 2015;13:2063–75.

[31] De Maeyer B, De Meyer SF, Feys HB, Pareyn I, Vandeputte N, Deckmyn H, et al. The distal carboxyterminal domains of murine ADAMTS13 influence proteolysis of platelet-decorated VWF strings in vivo. *J Thromb Haemost.* 2010;8:2305–12.

[32] Ono T, Mimuro J, Madoiwa S, Soejima K, Kashiwakura Y, Ishiwata A, et al. Severe secondary deficiency of von Willebrand

factor-cleaving protease (ADAMTS13) in patients with sepsis-induced disseminated intravascular coagulation: its correlation with development of renal failure. *Blood.* 2006;107:528–34.

[33] Yang S, Jin M, Lin S, Cataland S, Wu H. ADAMTS13 activity and antigen during therapy and follow-up of patients with idiopathic thrombotic thrombocytopenic purpura: correlation with clinical outcome. *Haematologica.* 2011;96:1521–7.

[34] Giavarina D. Understanding Bland Altman analysis. *Biochem Med.* 2015;25:141–51.

[35] Stephenson J, Chapman K, Mohammed S, Zebeljan D, Ahuja M, Donikian D, et al. A multicenter evaluation of the Technoscreen ADAMTS13 activity semi-quantitative screening test for thrombotic thrombocytopenic purpura diagnosis and exclusion. *Int J Lab Hematol.* 2023;45:562–70.

[36] Daems D, Lu J, Delport F, Mariën N, Orbie L, Aernouts B, et al. Competitive inhibition assay for the detection of progesterone in dairy milk using a fiber optic SPR biosensor. *Anal Chim Acta.* 2017;950:1–6.

SUPPLEMENTARY MATERIAL

The online version contains supplementary material available at https://doi.org/10.1016/j.rpth.2023.102171